



## Study of the structure properties of Co-doped ZnO thin films grown by pulsed laser deposition

Ali A. Yousif<sup>1</sup>, Adawiya J. Haidar<sup>2,\*</sup>, Nadir F. Habubi<sup>3</sup>

<sup>1</sup>*Department of Physics, College of Education, University of Al-Mustansiriyah, Baghdad/ Iraq.*

<sup>2</sup>*School of Applied Sciences, University of Technology, Baghdad/ Iraq.*

<sup>3</sup>*Department of Physics, College of Education, University of Al-Mustansiriyah, Baghdad/ Iraq.*

Received 8 June 2010; Revised 10 March 2011; Accepted 29 April 2011

### Abstract

We report the fabrication of Co-doped ZnO thin films prepared by Pulsed Laser Deposition (PLD) on glass substrates by Nd-YAG Q-Switching second harmonic generation (SHG) Pulsed Laser with a wavelength of 532nm, repetition rate of 10 Hz and pulsed width 10ns. The effect of doping on the structure properties of the ZnO:Co films have been investigated by X-Ray diffraction (XRD) and scanning electron microscopy (SEM). The result showed that polycrystalline and (100)-oriented pure ZnO films were obtained at all substrate temperature of (200°C and 400°C), laser fluence (0.4) J/cm<sup>2</sup> and the ZnO films grown at 400°C. X-ray diffraction (XRD) analysis demonstrates that the ZnO thin films with Co of (1, 3 and 5) wt.% have a highly (100) preferred orientation with only one high intense diffraction peak with a full width at half maximum (FWHM) less than 0.3°. The smallest grain size was obtained at scanning electron microscopy (SEM) in case of doping compared by grain size of XRD, while the polycrystalline grain size increased from 32.7 nm to 43.5 nm for pure ZnO films.

**Keywords:** Co-doped ZnO; Pulsed Laser Deposition; U.V emission; XRD.

**PACS:** 77.55.hf; 81.15.Fg; 79.60.Fr; 61.05.C-.

### 1. Introduction

Zinc oxide (ZnO) has been shown to exhibit the large direct band gap (3.37 eV) and exciton binding energy (60 meV) as well as the excellent chemical and thermal stability, properties that may lead to the important applications of this material in the ultraviolet devices, catalysis, piezoelectrics, and gas sensors [1-5]. Different deposition techniques are used to fabricate ZnO films including electrochemical deposition (ECD) technique [6], thermal oxidation [7], r.f. magnetron sputtering [8], pulsed laser deposition (PLD)[9]. PLD offers many advantages compared with other techniques: reduced contamination due to the use of laser light, control of the composition of deposited structure and in situ doping [10].

In this study we prepared Co-doped ZnO thin films deposited by PLD on glass substrates at 200°C and 400°C temperature. We also investigated the influence of laser (0.4)

---

\*) For Correspondence; Email: [adawiya\\_haider@yahoo.com](mailto:adawiya_haider@yahoo.com).

$J/cm^2$  applied during the deposition process on the structural and morphological properties of the films.

## 2. Experimental details

ZnO: Al<sub>2</sub>O<sub>3</sub> thin films sintered target of high – purity 99.99% was mounted in a locally design vacuum chamber and ablated by a double frequency with Q-switched Nd: YAG pulsed laser operated at 532 nm, pulse duration of about 10 ns, and a (0.4)  $J/cm^2$  energy density was focused on the target to generate plasma plume..

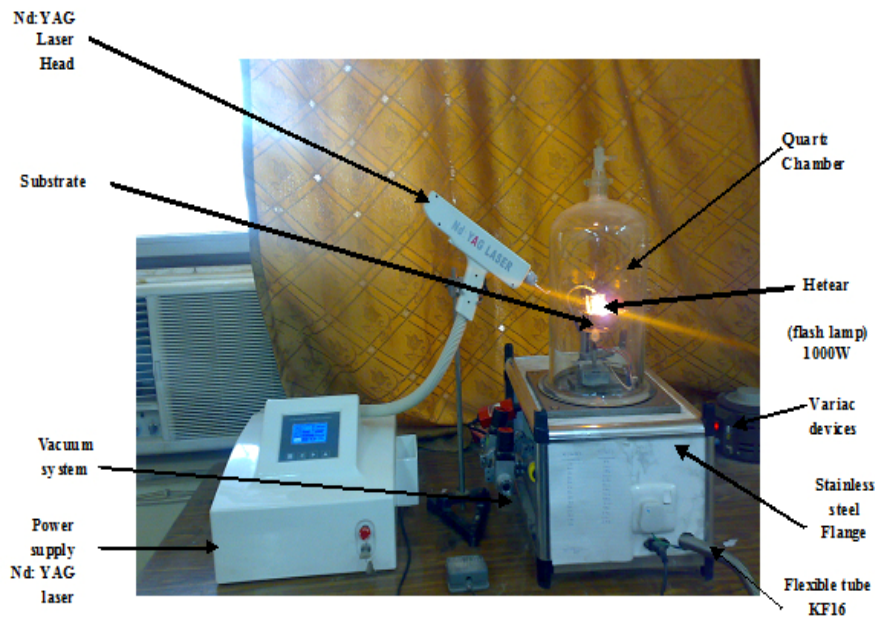


Fig. 1: Pulsed laser deposition (PLD) system

Amorphous fused silica (commercial available from Alfa Aesar) was used as substrates thin films were grown in Oxygen environment with O<sub>2</sub> partial pressure of 10<sup>-1</sup> mbar at substrate temperature of 400<sup>0</sup>C and 200<sup>0</sup>C). The deposition thin films were grown typically 10 min after the deposition thin films were cooled to room temperature.

X-ray powder diffraction (XRD) is one of the most powerful techniques for qualitative and quantitative analysis of crystalline compounds. This experimental technique has long been used to determine the overall structure, including lattice constants, identification of unknown materials, orientation of single crystals, orientation of polycrystals, defects, stresses, etc. In this study X-ray diffractometer type SHIMADZU, power diffraction system with Cu-K $\alpha$  x-ray tube ( $\lambda = 1.54056 \text{ \AA}$ ) was used. The x-ray scans were performed between 2 $\theta$  values of 30 $^\circ$  and 38 $^\circ$ . The morphological features of the various films were investigated with a JEOL JSM-6360 SEM equipped with an EDAX detector. The SEM is used in its common mode, the emission mode. In this mode, electrons fired from a filament (tungsten hairpin or LaB6) are accelerated with a voltage in the range of 1-30 kV down the center of an electron-optical column consisting of two or three magnetic lenses.

### 3. Results and Discussion

#### 3.1 Effect of Substrates Temperatures of pure ZnO films

The XRD pattern of pure ZnO target films prepared by pulsed laser deposition show polycrystalline structure of hexagonal wurtzite phase. The patterns of pure ZnO at different temperatures (200°C and 400°C). The films exhibit a dominant peak on  $2\theta = 31.7^\circ$  corresponding to the (100) plane of ZnO at 200°C and peak on  $2\theta = 31.748^\circ$  at 400°C, and other peaks corresponding to (002) and (101) indicating the polycrystalline nature of the films. The intensity of XRD peaks is related to many factors, which include crystallization quality, density, and thickness of thin films. The intensities of ZnO (100) peaks in XRD spectra are different due to the diverse crystallization quality and various substrate temperatures in spite of the same deposition condition [11].

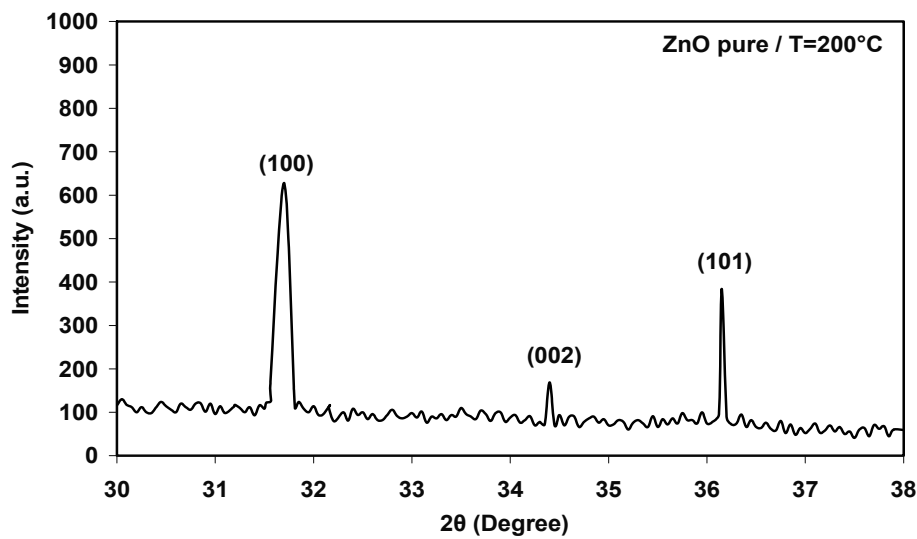


Fig. 2: XRD patterns of pure ZnO films grown on glass substrates at temperature 200°C.

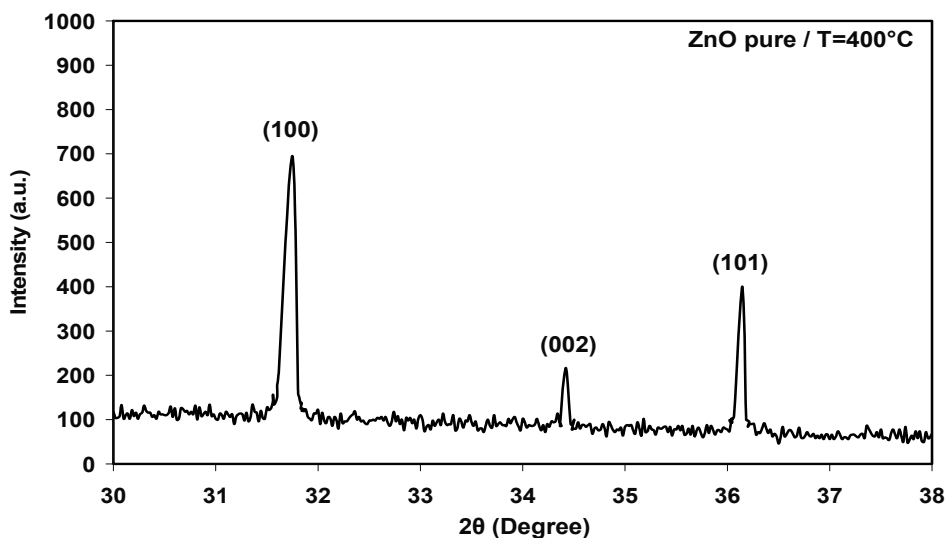


Fig. 3: XRD patterns of pure ZnO films grown on glass substrates at temperature 400°C

We can see that the film quality improved with increase temperature. This is because the atoms at lower temperatures do not have enough energy to locate their right positions [12]. It is seen from the figure that the relative intensity of the (100) peak increases with increasing temperature. The increase in peak intensity indicates an improvement in the crystallinity of the films with increase in grain size [13].

### 3.2 Effect of doping on pure ZnO films

The XRD patterns of ZnO and ZnO:Co films with different doping concentrations . as can be seen from this data, the structure of all the films are hexagonal with a strong (100) preferred orientation. No diffraction peaks of Co or other impurity phases are found in these samples. The angle of the dominant peak corresponding to (100) plane is at  $2\theta=31.7^\circ$  for the undoped ZnO sample, and it was increased as the concentration of Co impurity increased.

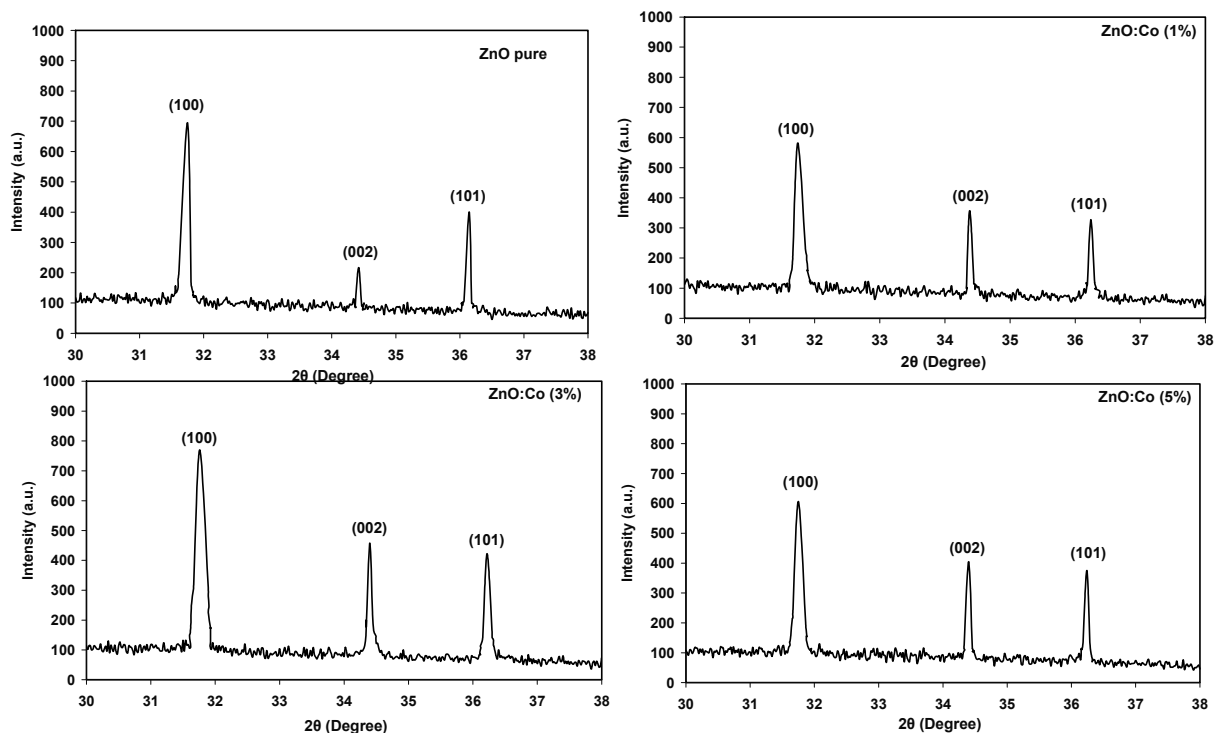


Fig. 4: XRD spectrum of ZnO pure and cobalt-doped ZnO thin films Deposited on glass substrate.

The calculated  $c$  values are found to decrease from 5.3 Å for ZnO films (undoped) to 5.21 Å for Co (5wt.%). The observed decrease in the  $c$  parameter may arise from the possible introduction of Co ions into interstitial sites [14], It is to be noted that the intensities of the characteristic peaks increase with increasing Co concentration of 3wt.%, however, some decrease in the intensities are observed for the Co concentration of about (1wt.%) and (5wt.%).

To compare our results with those given in the (ASTM data card 5-0664), one could conclude that the deposition films show a hexagonal structure of ZnO. Significant changes, observed in the X-ray diffraction patterns, manifest themselves in increase of peak intensity

corresponding to (100) crystal plane and a decrease in the peak intensity corresponding to other planes.

The lattice constants and the relative intensity ratio, [I (100)] in the diffraction pattern of undoped ZnO films deposited under various doping concentration are given in table (1). The lattice constants obtained are found to be in good agreement with ASTM data 5-0664 powder ZnO sample.

Table 1: Lattice constants and interplanar spacing as a function of undoped ZnO, ZnO:Al<sub>2</sub>O<sub>3</sub> and ZnO:Co thin films of various doping concentration.

| Sample                 | Investigated line | 2 $\theta$ | $\theta$ | d Å   | a. Å  | c. Å  |
|------------------------|-------------------|------------|----------|-------|-------|-------|
| ASTM                   | 100               | *          | *        | 2.816 | 3.249 | 5.205 |
| ZnO-pure<br>T=200°C    | 100               | 31.7       | 15.85    | 2.812 | 3.247 | 5.234 |
| ZnO-pure<br>T=400°C    | 100               | 31.748     | 15.87    | 2.813 | 3.248 | 5.300 |
| ZnO:Co (1%)<br>T=400°C | 100               | 31.74      | 15.87    | 2.813 | 3.248 | 5.216 |
| ZnO:Co (3%)<br>T=400°C | 100               | 31.76      | 15.88    | 2.814 | 3.249 | 5.099 |
| ZnO:Co (5%)<br>T=400°C | 100               | 31.75      | 15.87    | 2.815 | 3.250 | 5.210 |

The results of the (FWHM) for all samples point that they have values close together for undoped ZnO and ZnO:Co thin films of various doping concentration and increase for higher temperature for undoped ZnO. For Co concentration (1%, 3% and 5%) value is about (0.12° -0.15°) while for undoped it is about (0.25° -0.27°) as in table (2).

The average grain size ( $G_s$ ), which can be estimated using the Scherrer's formula (1) [15], the values of average grain size listed in the Table (2) show a decrease with at higher temperature for undoped ZnO, and a decreased when the concentration of Co was increased at doped rate (1 at.%- 5 at.%).

Table 2: The Size – strain data of investigated thin films

| Sample                    | Investigated line | FWHM (deg) | Grain size g.s (nm) | Integral Breadth $\beta$ | Shape factor $\Phi$ | Strain $\delta$ (%) | Stress $\sigma$ | Texture Coefficient $T_c$ (h k l) |
|---------------------------|-------------------|------------|---------------------|--------------------------|---------------------|---------------------|-----------------|-----------------------------------|
| ZnO-pure<br>T=200°C       | 100               | 0.270      | 31                  | 0.131                    | 2.06                | 9.122               | - 0.0804        | 1.7                               |
| ZnO-pure<br>T=400°C       | 100               | 0.254      | 33                  | 0.190                    | 1.33                | 9.167               | - 0.0808        | 1.68                              |
| ZnO:Co<br>(1%)<br>T=400°C | 100               | 0.138      | 60                  | 0.203                    | 0.67                | 9.167               | - 0.0808        | 1.39                              |
| ZnO:Co<br>(3%)<br>T=400°C | 100               | 0.120      | 69                  | 0.200                    | 0.60                | 9.212               | - 0.0812        | 1.41                              |
| ZnO:Co<br>(5%)<br>T=400°C | 100               | 0.156      | 54                  | 0.207                    | 0.75                | 9.258               | - 0.0816        | 1.32                              |

$$G_s = \frac{K\lambda}{\beta \cos \theta} \quad (1)$$

Where k: constant dependent on crystallite shape (0.94),  $\lambda$ : is the x-ray wavelength (1.54Å),  $\theta$ : Bragg diffraction angle of the XRD peak (degree) and  $\beta$  (radian) were determined from the broadening of the ZnO:Co thin films diffraction line. The values of the main Grain size from x-ray pattern of thin films are given in Table (2).

The integral breadth of the ZnO:Co thin films were obtained from the XRD pattern sheets using the relation (2), [16] our results indicate that  $\beta$  increase at higher temperature for undoped ZnO and increased for doping concentration for both Co, the value of  $\beta$  were shown in table (2).

$$\beta = \frac{Area}{I_o} \quad (2)$$

Where:

Area = area under peak and  $I_o$  = maximum intensity.

The shape factor was calculated of the samples using the relation (3) [16], the results show that the shape factor decreased with increasing temperature for undoped and doped in all concentration rates.

$$\Phi = \frac{\Delta}{\beta} \quad (3)$$

The microstrain depends directly on the lattice constant [17], and its value related to the shift from the ASTM standard value which could be calculated using the relation (1). No important effect of pure ZnO and various doping Co concentration for cobalt were recorded on the *c*-parameter, as seen in table (2).

The residual stress with decreasing the temperature increases for pure ZnO and for all the doping concentration. The values of the residual stress for undoped ZnO and ZnO:Co thin films were given in Table (2). The stress is negative, so the biaxial stress is compressive [18].

Texture coefficient ( $T_c$ ) of fabricated ZnO:Co thin film was calculated using relation (4). The results indicate that ( $T_c$ ) decrease with increasing doping for Co concentration. This is a usual result because increased doping causes an increase in the surface roughness. This result is in a good agreement with that in the Joseph [19].

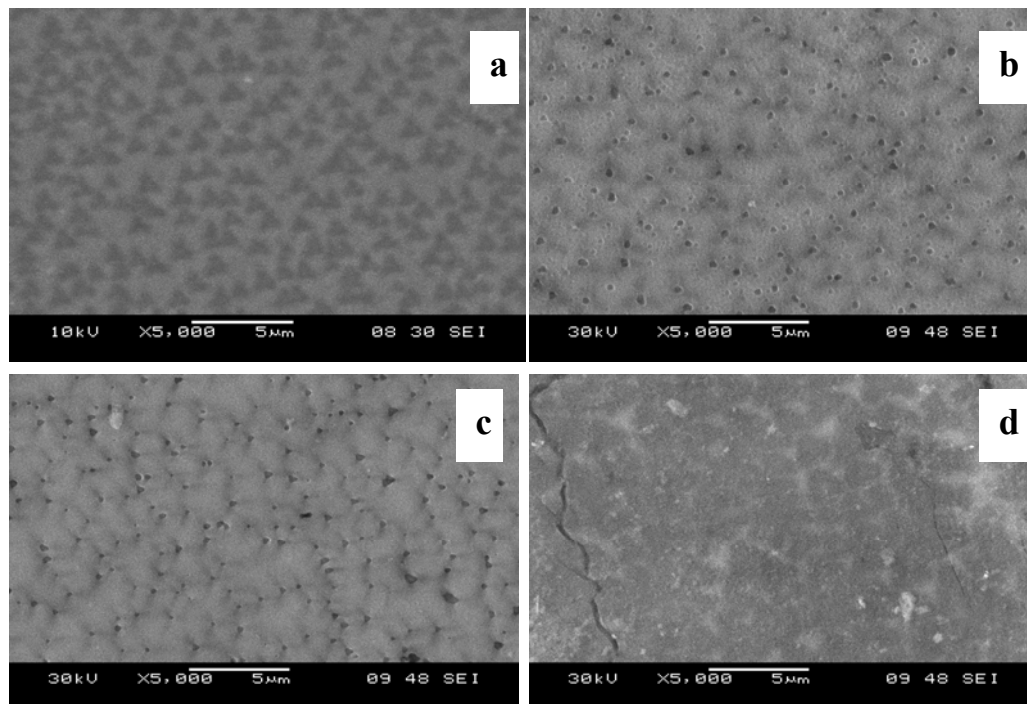
$$TC(hkl) = \frac{[I(hkl)/I_o(hkl)]}{[Nr - 1 \sum I(hkl)/I_o(hkl)]} \quad (4)$$

where *I* is the measured intensity, *I<sub>o</sub>* is the ASTM standard intensity, *Nr* is the reflection number and (hkl) is Miller indices.

#### 4. Surface morphology by (SEM)

##### 4.1 Effect Doping Concentration

A typical SEM image of the pure ZnO and Co-doped ZnO thin films respectively, deposited on glass substrates temperature of 400°C by pulsed laser deposition technique, 0.4 J/cm<sup>2</sup> laser energy and 10<sup>-1</sup> mbar Oxygen pressure. The surface is very smooth and the crystallites are very fine. No big particles can be found from SEM image. The grain size is ~ (34-67) nm. It is found that the Co doping concentration has a significant influence on ZnO film surface structure. The grain size increases as the Co concentration increases. The average grain size deduced from x-ray diffraction using the Scherer's formula is estimated at ~ (33-70) nm.



Figures 5: SEM images for pure ZnO and Co-doped ZnO thin films thin films (a) undoped, (b) 1 at.% Co, (c) 3 at.% Co, and (d) 5 at.% C

Therefore, XRD data reveal that the grain size was larger than that estimated from that obtained by SEM surface micrograph for Co doping concentration (see table 3). The grains become densely unpacked near regularly. The SEM micrographs showing the surface of ZnO films with various Co content are shown in Figures (5). The Co-free ZnO film displays hexagonal shaped films with submicron size diameter. As can be seen from the data of Figures (5), the addition of Co had limited the influence of the film morphology. 1 at. % Co in ZnO resulted in almost the same film shape as Co-free material, but the diameter of the films slightly increased. However, the diameter of the films decreased upon further increasing the Co concentration.

Table 3: Structural and morphological characteristics of the ZnO (undoped and Co doped) films deposited at 400 °C substrate temperature 0.4 J/cm<sup>2</sup> laser energy and 10<sup>-1</sup> mbar Oxygen pressure.

| Sample      | x-ray of plane<br>grain size<br>[nm] | SEM of plane<br>grain size<br>[nm] |
|-------------|--------------------------------------|------------------------------------|
| ZnO-pure    | 33                                   | 44                                 |
| ZnO:Co (1%) | 60                                   | 50                                 |
| ZnO:Co (3%) | 69                                   | 67                                 |
| ZnO:Co (5%) | 54                                   | 34                                 |



## 5. Conclusion

ZnO:Co thin films were deposited on glass substrate by Pulsed Laser Deposition at 200°C and 400°C temperature and at  $10^{-2}$  mbar oxygen background gas. The structural properties are found to be dependent on the laser fluence and temperature. The crystal structure of the films is hexagonal wurtzite. All films are polycrystalline and (100) oriented. This may be due to different effects, but the most relevant are grain size. From SEM the average grain size is roughly estimated to be (33.3-66.6) nm, were SEM studies indicate that the average grain size decreases with increase in dopant concentrations Co Films compared with XRD and increase in the of pure ZnO films. The strongest UV emission (around 378 nm) the full width at half maximum (FWHM) values of (100) peaks are (0.12°-0.27°).

## References

- [1] Z. W. Pan, Z. R. Dai, Z. L. Wang, *Journal of Crystal Growth, Science* **291** (2001) 1947
- [2] Z. R. Tian, J. A. Voigt, J. Liu, B. Mckenzie, M. J. Mcdermott, M. A. Rodriguez, H. Konishi, H. Xu, *Nature Mater.* **2** (2003) 1947
- [3] B. Liu, H. C. Zeng, *J. Am. Chem. Soc.* **126** (2004) 16744
- [4] M. H. Huang, S. Mao, H. Feick, H. Yan, Y. Wu, H. Kind, E. Weber, R. Russo, P. Yang, *Science* **292** (2001) 1897
- [5] Y. X. Wang *et al.* *Cryst. Res. Techno.* **44** (2009) 517
- [6] E. Gur, H. Asil, C. Cos, Kun, S. Tuzemen, K. Meral, Y. Onganer, K. Serifoglu, *Nucl. Instrum. Methods Phys. Res. B* **266** (2008) 2021
- [7] X. T. Zhang, Y.C. Liu, Z.Z. Zhi, J.Y. Zhang, Y.M. Lu, D.Z. Shen, X.W. Fan, X.G. Kong, *J. Lumin.* **99** (2002) 149
- [8] Q. P. Wang, X. J. Zhang, G.Q. Wang, S.H. Chen, X.H. Wu, H.L. Ma, *Appl. Surf. Sci.* **254** (2008) 5100
- [9] X. Q. Wei, Z. G. Zhang, M. Liu, C.S. Chen, G. Sun, C.S. Xue, H.Z. Zhuang, B. Y. Man, *Mater. Chem. Phys.* **101** (2007) 285
- [10] R. Eason, *Pulsed laser Deposition of thin films Applications-led growth of functional materials*, John Wiley & Sons, Inc. (2007)
- [11] F. K. Shan, B. C. Shin, S.W. Jang, Y. S. Yu, *J. Eur. Cer. Soc.* **24** (2004) 1015
- [12] W. Zhao-yang, H. Li-Zhong, Z. Jie, S. Jie, W. Zhi-Jun, *Vacu.* **78** (2005) 53
- [13] P. Sagar, M. Kumar, R. M. Mehra, *Mater. Sci. Pol.* **23** (2005) 685
- [14] D. R. Uhlmann, H. K. Bowen, W. D. Kingery, *Introduction to Ceramics*, John Wiley & Sons Inc, New York (1976)
- [15] C. Gümüs, O. M. Ozkendir, H. Kavak, Y. Ufuktepe, *J. Optoelectr. Advan. Mater.* **8** (2006) 299
- [16] P. Šutta, Q. Jackuliak, *Mater. Struct.* **5** (1998) 10
- [17] T. Obata, K. Komeda, T. Nakao, H. Ueba, C. Tasygama, *J. Appl. Phys.* **81** (1997) 199
- [18] C. Li, X. C. Li, P. X. Yan, E. M. Chong, Y. Liu, G. H. Yue, X. Y. Fan, *Appl. Surf. Sci.* **253** (2007) 4000
- [19] B. Joseph, P. K. Manoj, V. K. Vaidyan, *Bull. Mater. Sci.* **28** (2005) 487